JOURNAL OF MATERIALS SCIENCE 33 (1998) 1441–1444

Preparation and optical properties of nanocrystalline $(C_6H_5C_2H_4NH_3)_2PbI_4$-doped PMMA films

N. KITAZAWA
Department of Materials Science and Engineering, National Defence Academy, 1-10-20 Hashirimizu, Yokosuka, Kanagawa 239, Japan
E-mail: nkita@cc.nda.ac.jp

Nanocrystalline $(RNH_3)_2PbI_4$-doped PMMA films were successfully fabricated on glass substrates by the spin-coating technique and subsequent annealing. X-ray diffraction spectra revealed that the $(RNH_3)_2PbI_4$ crystals dispersed as nanometre-sized crystals in the PMMA matrix. These films showed a strong exciton absorption band with narrow bandwidth, even at room temperature. The exciton absorption observed here could be attributed to the 6s to 6p transition of Pb^{2+}. The stability of the $(RNH_3)_2PbI_4$ crystal was improved by doping these crystals into a PMMA matrix. © *1998 Chapman & Hall*

1. Introduction

The non-linear optical effects of low-dimensional structures with quantum functions have attracted considerable interest due to the possibility of creating interesting optical devices. These low-dimensonal materials are applicable for use in optical switches with ultrafast response time due to the enhanced third-order non-linear optical susceptibility, $\chi^{(3)}$ [1]. The improvement of $\chi^{(3)}$ has been investigated extensively in the area of quantum-dot doped materials [2, 3]. In these materials, it has been revealed that a sharp size distribution and a large volume fraction of quantum-dots is required in order to achieve high $\chi^{(3)}$ values. Recently, several methods, such as ion implantation [4] and the sol–gel [5] technique, have been used for obtaining a high-density quantum-dot doped materials. However, it is very difficult to make a quantum-dot structures with a homogeneous size distribution. It is also difficult to make even two-dimensional quantum well structures by artificial methods such as molecular beam epitaxy (MBE) and metal organic chemical vapour deposition (MOCVD) technique, because of the mismatch of the lattice constant and thermal expansion coefficient between well and barrier layers.

On the contrary, the existence of ideal two-dimensional structures have been reported on self-organized layered perovskite compounds, $(RNH_3)_2PbX_4$ (X, halogen; R, alkyl group) [6]. Crystal structures of these compounds can be regarded as semiconductor/insulator multiple quantum well structures consisting of lead halide semiconductor layers sandwiched between organic insulator layers. These compounds form a stable exciton with large binding energy, even at room temperature [7, 8]. $(RNH_3)_2PbX_4$ crystals, therefore, have considerable potential for use in non-linear optical materials. However, the ordered two-dimensional structure is easily decomposed by moisture because of the hygroscopic property of these compounds. Degradation of crystals will be suppressed by doping the nanocrystalline $(RNH_3)_2PbX_4$ into a solid matrix with high transparency. In this study, the preparation and optical properties of nanocrystalline $(C_6H_5C_2H_4NH_3)_2PbI_4$-doped PMMA thin films were investigated.

2. Experimental procedure

Nanocrystalline $(C_6H_5C_2H_4NH_3)_2PbI_4$-doped PMMA thin films were prepared on an SiO_2 glass substrate by the spin-coating method at 2000 r.p.m. Poly(methylmethacrylate) (PMMA), RNH_3I (R, $C_6H_5C_2H_4$–) and PbI_2, were dissolved in *N*,*N*-dimethylformamide (DMF). The concentration of PMMA in DMF was 20 wt % and the weight ratio of $(RNH_3)_2PbI_4$/PMMA was 0.2. Spin-coated $(RNH_3)_2PbI_4$-doped PMMA thin films were then annealed at various temperatures for various times. Thin films of microcrystalline $(RNH_3)_2PbI_4$ were also prepared by the spin-coating technique using 2 wt % acetonitrile solution. These films were stored in a humidity-controlled (20%–30% RH) dry box.

The thicknesses of $(RNH_3)_2PbI_4$-doped PMMA thin films were estimated by using a surface roughness tester. The film thicknesses studied here were about 0.2 μm. Crystallinity and orientation of $(RNH_3)_2PbI_4$-doped PMMA thin films were determined from the X-ray diffraction spectra. Intensity data were recorded at room temperature (Rigaku, RINT2500 X-ray diffractometer) using monochromatic CuK_α radiation (40 kV, 30 mA). Optical absorption spectra of $(RNH_3)_2PbI_4$-doped PMMA thin films on glass

substrates were measured using a conventional UV–VIS spectrometer (Hitachi, U-1100 spectrophotometer) at room temperature. Note that the incident light beam is kept perpendicular to the substrate surface.

3. Results and discussion

Fig. 1 shows the optical absorption spectra of (a) polycrystalline $(RNH_3)_2PbI_4$ film and (b) $(RNH_3)_2PbI_4$-doped PMMA film measured at room temperature. Note that annealing temperature and time of the $(RNH_3)_2PbI_4$-doped PMMA film are 125 °C and 10 min, respectively. In the spectra of $(RNH_3)_2PbI_4$ film shown in curve (a), a strong absorption band with narrow bandwidth ($\sim$70 meV) was observed at 2.4 eV. This absorption band has been attributed to the exciton of $(RNH_3)_2PbI_4$ crystal which was formed by the transition from Pb^{2+}(6s) to Pb^{2+}(6p) [9]. The fundamental transition from Pb^{2+}(6s) to Pb^{2+}(6p) was also observed at around 2.7 eV. A spectrum similar to that for $(RNH_3)_2PbI_4$ film was obtained for $(RNH_3)_2PbI_4$-doped PMMA film shown in curve (b). The peak position and bandwidth of the exciton absorption band of $(RNH_3)_2PbI_4$-doped PMMA film were comparable to those of $(RNH_3)_2PbI_4$ film shown in curve (a). These results indicated that the $(RNH_3)_2PbI_4$ crystals were successfully doped into PMMA using the present technique.

Typical X-ray diffraction (XRD) spectra of (a) polycrystalline $(RNH_3)_2PbI_4$ film and (b) $(RNH_3)_2PbI_4$-doped PMMA film are shown in Fig. 2. As seen in curve (a), sharp (0 0 2l) (l = 2–4) diffraction peaks associated with $(RNH_3)_2PbI_4$ crystal were clearly observed. $(RNH_3)_2PbI_4$-doped PMMA film showed the same diffraction angles as $(RNH_3)_2PbI_4$ film. These XRD results revealed that $(RNH_3)_2PbI_4$ crystals precipitated in the PMMA matrix were highly oriented, with the c-axis perpendicular to the substrate surface.

Fig. 3 shows the change in the exciton absorption band of $(RNH_3)_2PbI_4$-doped PMMA films as a function of annealing time at various temperatures. In these spectra, strong exciton absorption bands due to the precipitation of $(RNH_3)_2PbI_4$ crystals were clearly observed. Moreover, the peak position of the exciton absorption band remained constant with change in annealing time and temperature. As shown in Fig. 3a, an exciton absorption band was observed at around 2.4 eV, and the absorption intensity increased with increasing annealing time. When $(RNH_3)_2PbI_4$-doped PMMA films were annealed at 150 °C (Fig. 3b), the exciton absorption intensity of these films rapidly decreased with increasing annealing time and then the exciton absorption band disappeared. From the XRD investigation shown in Fig. 4, the (0 0 1) diffraction peak associated with the precipitation of PbI_2 crystal was observed when the film was annealed at 150 °C for 60 min. Therefore, the decrease in the exciton absorption intensity of $(RNH_3)_2PbI_4$-doped PMMA films during annealing is consistent with the decomposition of $(RNH_3)_2PbI_4$ crystals.

The average size of $(RNH_3)_2PbI_4$ crystals precipitated in PMMA films are estimated from Scherrer's equation using the (0 0 12) X-ray diffraction peaks, and are plotted in Fig. 5 as a function of annealing time. As seen in this figure, the mean diameter of $(RNH_3)_2PbI_4$ crystals was estimated to be nanometre-sized. When the film was annealed at 100 °C, the diameter increased with increasing annealing time. At 125 °C, the average sizes of crystals increased with increasing annealing time and showed a maximum (60 nm); however, the size decreased on further annealing. A decrease in the average sizes of crystals with increasing annealing time was observed at 150 °C. This is due to the decomposition of crystals seen in Fig. 4.

The stability of the $(RNH_3)_2PbI_4$ crystal was estimated using optical absorption and XRD spectra. Fig. 6 shows the optical absorption spectra of (a) polycrystalline $(RNH_3)_2PbI_4$ film and (b)

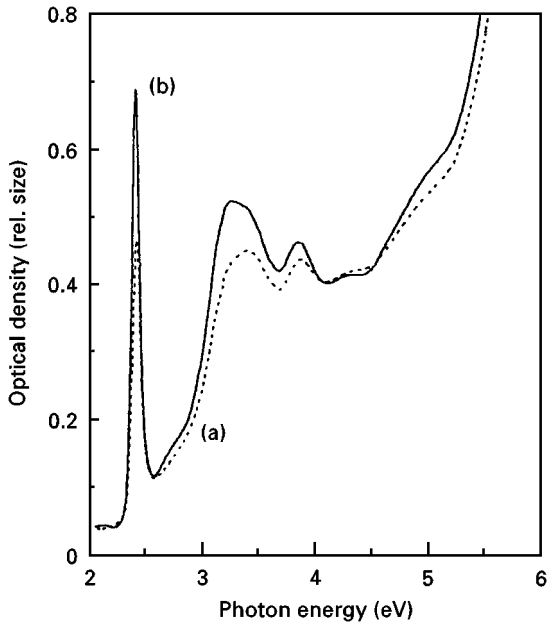

Figure 1 Optical absorption spectra of (a) $(C_6H_5C_2H_4NH_3)_2PbI_4$ and (b) $(C_6H_5C_2H_4NH_3)_2PbI_4$-doped PMMA films measured at room temperature. $(C_6H_5C_2H_4NH_3)_2PbI_4$-doped PMMA film was annealed at 125 °C for 10 min.

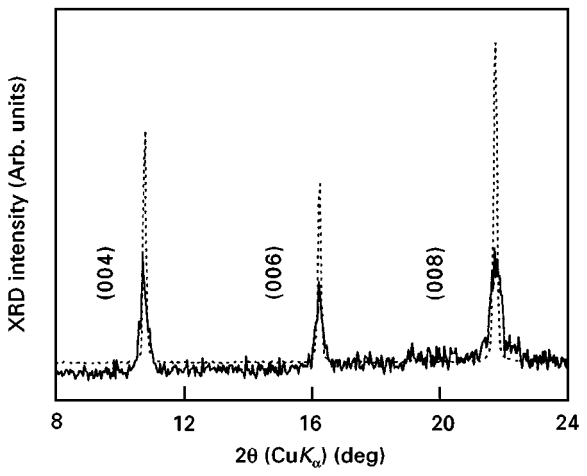

Figure 2 X-ray diffraction spectra of (– – –) $(C_6H_5C_2H_4NH_3)_2PbI_4$ and (——) $(C_6H_5C_2H_4NH_3)_2PbI_4$-doped PMMA films. The $(C_6H_5C_2H_4NH_3)_2PbI_4$-doped PMMA film was annealed at 125 °C for 10 min.

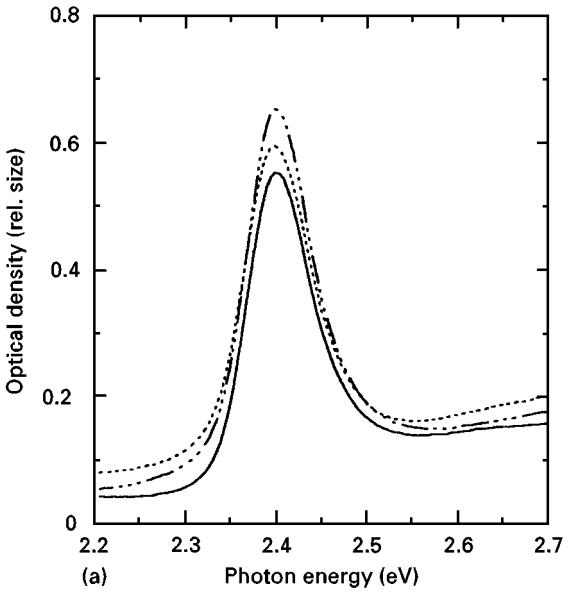

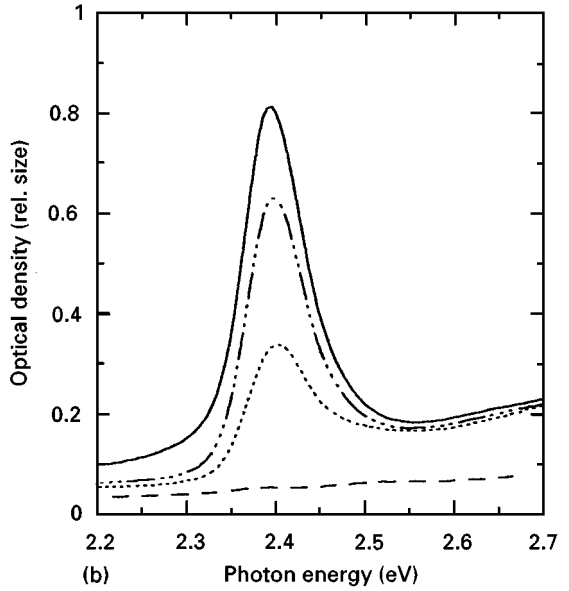

Figure 3 Change in the exciton absorption band of $(C_6H_5C_2H_4NH_3)_2PbI_4$-doped PMMA films as a function of annealing time. The annealing temperatures were (a) 100 °C and (b) 150 °C. (a) (——) 10 min, (— - - - —) 30 min, (- - - -) 60 min. (b) (——) 1 min, (— - - - —) 10 min, (- - -) 30 min, (– – –) 60 min.

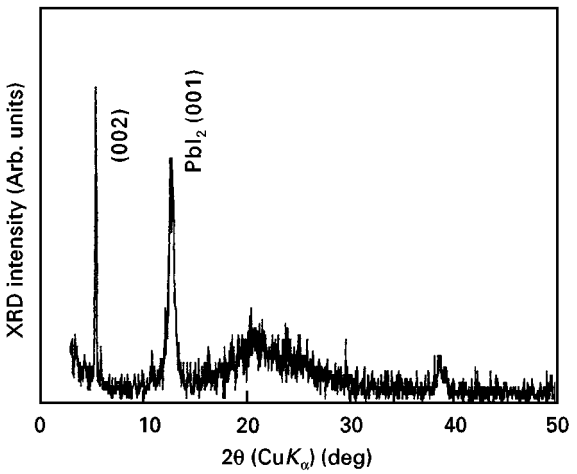

Figure 4 X-ray diffraction spectra of $(C_6H_5C_2H_4NH_3)_2PbI_4$-doped PMMA film annealed at 150 °C for 60 min.

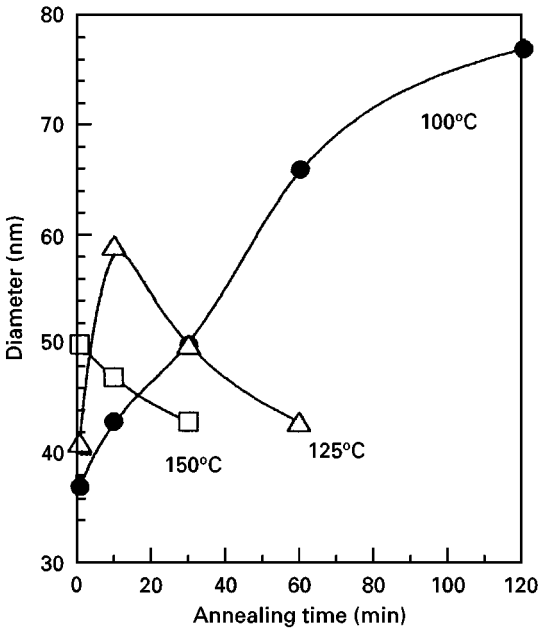

Figure 5 Change in the average sizes of $(C_6H_5C_2H_4NH_3)_2PbI_4$ crystals in PMMA films as a function of annealing time.

$(RNH_3)_2PbI_4$-doped PMMA film stored for 2 months in a humidity-controlled dry box. In the $(RNH_3)_2PbI_4$ film, curve (a), the strong exciton absorption peak disappeared and a new absorption band was observed at around 3.0 eV. This spectrum resembles the aniline intercalated PbI_2 [10]. In contrast, in the $(RNH_3)_2PbI_4$-doped PMMA film shown in curve (b), a strong exciton absorption band was clearly observed. From comparison with the spectrum of Fig. 1, the exciton absorption intensity of these films are seen to be comparable. Therefore, degradation of crystals could be suppressed by doping the nanocrystalline $(RNH_3)_2PbX_4$ into PMMA matrix. The above consideration is also supported by the X-ray diffraction spectra shown in Fig. 7. As seen in this figure, $(RNH_3)_2PbI_4$-doped PMMA film showed only (0 0 2*l*) diffraction peaks. This indicated that $(RNH_3)_2PbI_4$ crystal in PMMA film remained two-dimensional in structure. In $(RNH_3)_2PbI_4$ film, however, the (0 0 2*l*) diffraction peaks associated with $(RNH_3)_2PbI_4$ crystal were not observed. Although the crystal phase observed in $(RNH_3)_2PbI_4$ film is not precisely identified, amine–PbI_2 complex may be formed in this film.

In this study, preparation and optical properties of nanocrystalline $(C_6H_5C_2H_4NH_3)_2PbI_4$-doped PMMA films were investigated. Nanocrystalline $(RNH_3)_2PbI_4$-doped PMMA films were successfully fabricated on glass substrates from DMF solutions by the spin-coating technique and subsequent annealing. From the optical absorption measurements, $(RNH_3)_2PbI_4$-doped PMMA films studied here showed strong exciton absorption band with narrow ($\sim$70 meV) bandwidth even at room temperature. Regarding the optical transition, it is well known that the fundamental transition in $(RNH_3)_2PbI_4$ is similar to that in PbI_2 [7, 9]. In these compounds, the top of the valence band is composed

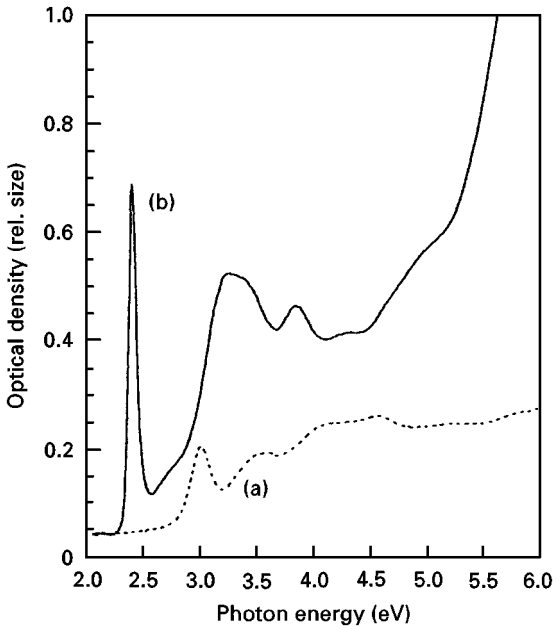

Figure 6 Optical absorption spectra of (a) $(C_6H_5C_2H_4NH_3)_2PbI_4$ and (b) $(C_6H_5C_2H_4NH_3)_2PbI_4$-doped PMMA films after 2 months. $(C_6H_5C_2H_4NH_3)_2PbI_4$-doped PMMA film was annealed at 125 °C for 10 min.

of the Pb(6s) orbital which is hybridized with the I(5p) orbital, and the bottom of the conduction band mainly has Pb(6p) character. As seen in Fig. 1, the exciton absorption and fundamental transition from valence to conduction band are observed at 2.4 and 2.7 eV, respectively. The exciton binding energy of $(RNH_3)_2PbI_4$-doped PMMA film was, therefore, estimated to be 300 meV. These values are very large compared with those of PbI_2 (30 meV), and are comparable to $(C_{10}H_{21}NH_3)_2PbI_4$ (320–370 meV) and $(C_6H_5C_2H_4NH_3)_2PbI_4$ (250 meV) [7, 9, 11–13]. From the results shown in Figs 3 and 4, there is no dependence between the peak position of the exciton absorption band and the average diameter of the crystals. This is due to the large crystal size compared with the Bohr radius of the exciton formed in $(RNH_3)_2PbI_4$ crystals (1.7 nm) [14]. Therefore, the enhancement of exciton binding energy observed for $(RNH_3)_2PbI_4$-doped PMMA films are also consistent with dielectric confinement effect. The degradation of the crystals could be suppressed by doping the nanocrystalline $(RNH_3)_2PbI_4$ into a PMMA matrix as shown in Figs 6 and 7. These results lead us to the strong belief that the $(RNH_3)_2PbI_4$-doped PMMA films can be of considerable potential for use in non-linear optical materials.

More detailed studies of nanocrystalline $(RNH_3)_2PbI_4$ formation and the measurement of their non-linear optical properties are being carried out.

4. Conclusions

The preparation and optical properties of nanocrystalline $(C_6H_5C_2H_4NH_3)_2PbI_4$-doped PMMA thin film were investigated. The following conclusions were drawn.

1. Nanometre-sized $(C_6H_5C_2H_4NH_3)_2PbI_4$-doped PMMA films were successfully fabricated on glass substrates from DMF solutions by the spin-coating technique and subsequent annealing.

2. $(C_6H_5C_2H_4NH_3)_2PbI_4$-doped PMMA films showed a strong absorption band with narrow bandwidth even at room temperature. This absorption band has been attributed to the exciton of $(RNH_3)_2PbI_4$ crystal which was formed by the transition from Pb^{2+}(6s) to Pb^{2+}(6p). The exciton binding energy was estimated to be about 300 meV.

3. The degradation of $(RNH_3)_2PbI_4$ crystals could be suppressed by doping the nanocrystalline $(RNH_3)_2PbI_4$ into a PMMA matrix.

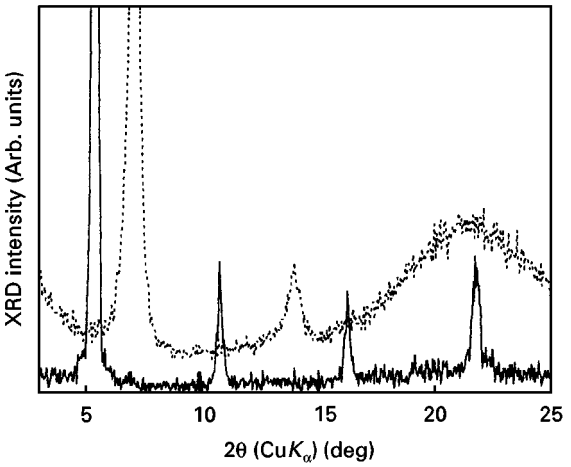

Figure 7 X-ray diffraction spectra of (– – –) $(C_6H_5C_2H_4NH_3)_2PbI_4$ and (——) $(C_6H_5C_2H_4NH_3)_2PbI_4$-doped PMMA film after 2 months.

References

1. D. RICARD, P. ROUSSIGNOL and C. FLYTZANIS, *Opt. Lett.* **10** (1985) 511.
2. N. KITAZAWA, T. YANO, S. SHIBATA and M. YAMANE, *Jpn J. Appl. Phys.* **35** (1996) 2228.
3. K. UCHIDA, S. AKNEKO, S. OMI, C. HATA, H. TANJI, Y. ASAHARA, A. J. IKUSHIMA, T. TOKIZAKI and A. NAKAMURA, *J. Opt. Soc. Amer.* **B11** (1994) 1236.
4. H. HOSONO and H. KAWAZOE, *Mater. Sci. Engng* **B41** (1996) 39.
5. J. M. F. NAVARRO and M. A. VILLEGAS, *Glastech. Ber.* **65** (1992) 32.
6. J. CALABRESE, N. L. JONES, R. L. HARLOW, N. HERRON, D. L. THORN and Y. WANG, *J. Amer. Chem. Soc.* **113** (1991) 2328.
7. T. ISHIHARA, J. TAKAHASHI and T. GOTO, *Solid State Commun.* **69** (1989) 933.
8. M. ERA, S. MORIMOTO, T. TSUTSUI and S. SAITO, *Appl. Phys. Lett.* **65** (1994) 676.
9. T. ISHIHARA, J. TAKAHASHI and T. GOTO, *Phys. Rev.* **B42** (1990) 11099.
10. V. MEHROTRA, S. LOMBARDO, M. O. THOMPSON and E. P. GIANNELIS, *ibid.* **B44** (1991) 5786.
11. T. ISHIHARA, X. HONG, J. DING and A. V. NURMIKKO, *Surf. Sci.* **267** (1992) 323.
12. L. C. TANH, C. DEPEURISINGE, F. LEVY and E. HOOSER, *J. Phys. Chem. Solids* **36** (1975) 699.
13. E. A. MULJAROV, S. G. TIKHODEEV, N. A. GIPPIUS and T. ISHIHARA, *Phys. Rev.* **B51** (1995) 14370.
14. X. HONG, T. ISHIHARA and A. V. NURMIKKO, *ibid.* **B45** (1992) 6961.

Received 6 May
and accepted 27 November 1997